CORONAL SUTURE MORPHOLOGY AND SYNOSTOTIC PROGRESSION IN RABBITS WITH DELAYED-ONSET CRANIOSYNOSTOSIS.

by

Harman Singh Deol

B.A. Anthropology, University of Pittsburgh, 2013

Submitted to the Graduate Faculty of

the School of Dental Medicine in partial fulfillment

of the requirements for the degree of

Master of Science

University of Pittsburgh

2017

UNIVERSITY OF PITTSBURGH

SCHOOL OF DENTAL MEDICINE

This thesis was presented

by

Harman Singh Deol

It was defended on

January 3, 2017

and approved by

Michael I Siegel, PhD., Professor, Department of Anthropology

Seth Weinberg, PhD., Associate Professor, Department of Oral Biology

Gregory M. Cooper, PhD., Assistant Professor, Department of Plastic Surgery, Oral Biology,

and Bioengineering

Thesis Director: Mark P. Mooney, PhD., Professor, Department of Oral Biology,

Anthropology, Plastic Surgery, Orthodontics, and Communication Science and Disorders

CORONAL SUTURE MORPHOLOGY AND SYNOSTOTIC PROGRESSION IN RABBITS WITH DELAYED-ONSET CRANIOSYNOSTOSIS

Harman Singh Deol, M.S.

University of Pittsburgh, 2017

Delayed-onset craniosynostosis has been reported in the human clinical literature and may represent part of the expanded phenotype of craniosynostosis. Delayed-onset synostosis (DOS) is also an integral part of the phenotypic spectrum in an inbred rabbit strain of craniosynostosis. The purpose of the present study was to qualitatively and quantitatively describe the perisynostotic events in the coronal sutures of rabbits with delay-onset coronal suture synostosis compared to age matched, wild-type control rabbits.

Coronal sutures from 80 rabbits (39 normal wild-type controls and 41 DOS) were collected for gross morphological and histological examination. Ages ranged from term (day 0) through 88 days of age. The sutures were harvested, formalin fixed, paraffin embedded, and stained with alizarin red for gross light microscopic analysis.

Qualitative results showed that by 25 days of age a dramatic thickening of the sutural ligament, an increase in the amount of bone in the osteogenic fronts, and an increase in the frequency of bony bridges between the frontal and parietal bones in rabbits with DOS compared to age matched, wild-type controls. No statistical significant differences in mean suture width or total suture area between the groups at the interdigitating zone were recorded at any age and

cortical level (p> 0.05). At a region of the coronal suture closer to the midline, deemed the

medial zone, a significant difference was found in mean suture width between groups at 88 day

in age group at the ectocortical suture surface (p <.05); additionally, significant differences in

mean suture area between the groups were recorded at age 25 and 88 (p <.05). A significant

difference bony bridging frequency between the interdigitating zone and medial zone of DOS

sutures was observed at the 45 day age group. The results of the 6X2 (age by group) two-way

ANOVA indicate significant interaction at various cortical levels as well as total suture area at

the interdigitating and medial zone (p < 0.05).

Results suggest that bony bridging and sutural ligament thickening occurs much earlier

than coronal suture growth cessation in DOS rabbits and that these factors may limit subsequent

sutural growth in an additive effect.

TABLE OF CONTENTS

LIST OF TABLES

LIST OF FIGURES

PREFACE

I would like to acknowledge the Department of Anthropology for the support that I received while working in the physical anthropology laboratory and completing my coursework for the Oral Biology program. I am privileged to have worked with a great variety of individuals ranging from interns, staff, and faculty of the department, and believe that my experience was shaped by those I interacted with.

I would like to thank Dr. Siegel, Dr. Weinberg, and Dr. Cooper for their continual motivation for me to work at a high level and for being members of my thesis committee. Your time and flexibility has been vital as I worked through this process to completion.   I am also grateful for all of my professors and colleagues from the Oral Biology department that I have had the opportunity to learn from during my time in the program.

I have been extremely lucky to work along side Dr. Mooney for the past 5 years. Your knowledge as a professor and guidance as an advisor has been monumental to my pursuit of a life in science. As a boss you taught me that confidence and humility are key in working in collaborative setting. I appreciate everything you have done for me and will take the lessons you taught with me as I progress through the various stages of my education and career.

Lastly, I would like to thank my parents and family. Your love has and support has shown no limits.

1.0   INTRODUCTION

During embryonic development, craniofacial bones arise through intramembranous and endochondral processes. Skull bones arising from such development, grow from a central location peripherally, with articulations forming between the bony plates. Skull sutures are a thin layer of fibrous tissue found at the articulations of approximating bones (Cohen, 2000). Collagen, the predominant fibrous constituent of postnatal skull sutures, arrange between adjacent bones to resist tensile or compressive forces (Herring, 2000, 2008). Development of the sutural joint is formed by cell division and growth of cells at extensions, called osteogenic fronts, of each adjacent skull bone (Cohen, 2000). Functioning sutures allow for continuous growth of the cranial vault, with bone deposition and reposition occurring at the osteogenic fronts of neighboring skull bones present at the suture (Cohen, 2000). Such articulations are present in the neurocranium between the parietal bones, at the sagittal suture, the parietal and frontal bone, at the coronal suture, and the the parietal and occipital bone, at the lambdoid suture (Cohen, 2000).

In craniosynostosis, premature closure of skull sutures is observed (Cohen, 2000). Under this condition, the formation of patent suture occurs, however, early obliteration follows (Cohen, 2000; Mooney et al., 1994a). In cases of craniosynostosis, fusion begins at a localized region, deemed the zone of complete osseous obliteration, and moves medial and laterally along the suture (Cohen, 2000). In the rabbit model, the zone of complete osseous obliteration has served

as a synostoic foci and corresponds with underlying dural sinus tracts (Mooney et al, 2007; Reed et al, 2007). On gross morphological description of this region, extensive interdigitating of the coronal suture and bony bridging between frontal and parietal osteogenic fronts has been described. (Mooney et al, 1996). In this study, the interdigitating zone was studied as a potential initiation focus for suture fusion. Additionally, a region medially located (near the sagittal suture), was studied as a means to track synostotic progression along the width of the suture; this region has been named the medial zone.

It is estimated that nonsyndromic craniosynostosis affects 300 per 1 million births, of which 24% are affecting the coronal suture (Cohen 1986). In humans, the coronal suture typically is expected to remain patent throughout the stages of brain development and only begin physiological fusion between 22 and 39 years of age (Cohen, 1993). Normal brain growth typically plateaus around 6 yeas of age. Instances of isolated delayed onset coronal suture synostosis occurring before the age of 6 would severely limit normal expansion of the cranial vault and result in impeded brain growth and development. Due to the compensatory growth along perpendicular axis to the affected suture, craniometrics and analysis of an affected individual's head shape has allowed for definitive diagnosis of suture fusion (Cunningham and Heike, 2007). Additionally, approximately 150 syndromes have been identified causing primary or secondary premature suture fusion, including Apert syndrome, Carpenter syndrome, Crouzon syndrome, Saethre-Chotzen syndrome, Pfeiffer syndrome, as well as others (Rogers et al., 2015; Cohen, 2000c, Connolly et al., 2004, Hoefkens et al., 2004).

Though many syndromic causes of primary or secondary craniosynostosis have identified gene mutations, environmental etiologies, including in-utero growth restrictions and metabolic disorders, have been associated with craniosynostosis (Cunningham and Heike, 2007; Graham et al., 1980). Nonsyndromic single suture fusion has been identified as the most common form of craniosynostosis, however, the pathogenesis of premature suture fusion is not well understood. (Cunningham and Heike, 2007; Cohen, 2000; Johnson and Wilkie 2011). Mutations in *FGFR2*, *FGFR3, TWIST, MSX2,* and *TGFβR* genes have been implicated as potential etiologies of coronal suture fusion (Renier et al., 2000; Reardon et al., 1997; Seto et al., 2007; Johnson et al., 2000). Additionally, growth factors, such as Tgf-β isoforms, secreted by the dura mater have been reported as integral components of maintaining normal suture physiology (Poisson et al., 2004; Johnson and Wilkie, 2011). Recently, Tgf-β2 neutralizing antibody was successfully used to rescue coronal sutures in DOS rabbits, indicating the role of molecular signals in suture fusion and the potential of cytokine therapy (Mooney et al., 2016).

In 1994, a rabbit colony expressing nonsyndromic coronal suture craniosynostosis was reported (Mooney et al., 1994a). This model has been valuable in describing the pathological progression of early suture fusion, which can be applied in syndromic and nonsyndromic cases (Mooney et al., 1994a). In early descriptions of the rabbit model, trends suggested the trait followed an autosomal dominant inheritance pattern with high penetrance and variable expression of the disorder (Mooney et al., 1994a). Phenotypically, early and delayed onset synostosis has been observed both bilaterally or unilaterally across the coronal suture in the affected rabbit population. In early onset bilateral coronal synostosis, affected animals exhibited brachycephaly, elevated bony coronal ridging, frontal bossing, and a domed appearance in the

anterior cranial vault (Mooney et al., 1994a). The delayed onset synostosis rabbits showed many of the same features, though phenotypically milder (Mooney et al., 1994a). Additionally, it is important to note that the early onset phenotype rabbits have obliterated sutures by term, while patent sutures exist in rabbits of the delayed onset phenotype at term.

In a follow up study, radiopaque markers were placed anteriorly and posteriorly to the coronal sutures of rabbits within the colony. In this study, marker separation was tracked at various time points radiographic analysis and measurements (Mooney et al., 1994b). Across the 18-week study, completely synostosed sutures showed a 90% reduction in coronal suture growth when compared to unaffected suture growth, and partially synostosed sutures showed a 25% reduction of coronal suture growth (Mooney et al., 1994b). In this study, variable expression of craniosynosostosis within the affected population was observed, however, key similarities in growth patterns suggest a link between the morphology of progression of synostosis between the complete and partial.

A histological analysis of the coronal sutures of the complete synostosis rabbits was conducted and revealed that suture fusion began at a region in the middle of the suture, also called the interdigitating zone (Mooney et al., 1996). Osseous projections connecting the osteogenic fronts of the parietal and frontal bones were detected earliest at the interdigitating zone and progressed medially and laterally, eventually leading to complete suture obliteration (Mooney et al., 1996). It is important to note that these animals did show the formation of a suture, however, thick osteogenic fronts, extensive bony bridging, and suture fusion appeared prenatally (Mooney et al., 1996).

A gross morphological description of partially synostosis rabbits, also called delayed-onset synostosis rabbits (DOS), has been conducted and the results, as described earlier, have been published (Mooney et al., 1998, 1996). The DOS rabbits show plateauing of coronal suture growth followed by suture obliteration by 42 days of age. Additionally, human cases of delayed onset synostosis have been reported (Cohen et al., 1993; Reddy et al., 1990). Using the delayed onset phenotype, studies testing potential therapies for abnormal suture fusion can be conducted significantly easier. However, a histologic description of the progression of suture closure in this phenotype has not been performed to determine if the delayed onset group serves as a proper model for other phenotypes.

2.0   HYPOTHESIS

The objective of this study is to describe the progression of coronal suture synostosis in DOS rabbits against wild type controls through histological analysis. Though initial development of a patent suture will be observed in the sutures of the affected group, suture fusion is expected by day 88. Dysmorphic suture features such as end to end articulation of the osteogenic fronts and bony bridging may indicate the progression of synostosis in the affected group at the interdigitating and medial zone. Additionally, it is hypothesized that a significant difference in mean suture width and total suture area will be measured between the DOS affected group. Through both qualitative and quantitative analysis, bony bridging is expected to be seen at first at the interdigitating zone, a region laterally located along the width of the suture, and at the medial zone in older rabbits within the affected group. Sutures in the wild type control are anticipated to remain patent at all ages.

3.0 MATERIALS AND METHODS

3.1 SAMPLE COLLECTION AND HISTOLOGICAL STAINING

The calvaria from 80 postnatal New Zealand White rabbits (*Orcyctolagus cuniculus*) were examined in this study. Sutures were collected from rabbits 1, 5, 10, 25, 31, 42, 88, 150 age in days (Table 1). Of the samples collected, 39 were unaffected wild type controls and 41 were delayed onset craniosynostosis rabbits.

Rabbits were euthanized with an overdose of penobarbital (Nembutal, 300mg/kg, IV; Abbot Labs, Chicago, IL). Following the sacrifice, suture status was diagnosed by visual observation (Mooney et al. 1994a 1996) as unaffected or delayed onset. The sutures of the rabbits were harvested from the calvaria in rectangular blocks (160 total sutures) and processed for serial histologic examination. The sutures were fixed in 10% buffered neutral formalin, demineralized in 5% trichloroacetic acid (TCA), dehydrated in a series of acetone washes, and embedded in mehtylmethacrylate (JB-4 Plus, Polyscience, Inc., Warington, PA). The specimens were then sectioned with a thickness of 5 microns (μ) along the sagittal plane of the coronal suture. The sections were then treated and stained with hematoxylin and erythrosine for light microscopy and histomorphometric analysis.

Table 1 Sample Size Qualitative Analysis- The number of animals used by age and group for the qualitative

analysis

	Age (Days)								Total Subjects	Total Sutures
	1	*5*	*10*	*25*	*31*	*42*	*88*	*150*		
Wild Type	11	6	5	5	3	3	4	2	39	78
DOS	8	7	4	5	3	5	5	4	41	82

Table 2 Sample Size Quantitative Analysis- The number of sutures by age and diagnosis group used for

quantitative analysis (suture width, total suture area, and bony bridging frequency).

	Age (Days)						Total Sutures
	5	*10*	*25*	*31*	*42*	*88*	
Wild Type	3	1	2	1	2	2	11
DOS	2	2	3	2	4	2	15

3.2   MICROSCOPY AND METRIC COLLECTION

Histological slides were qualitatively and quantitatively analyzed using a Leica MZ12 Stereo Zoom microscope and Northern Eclipse (v 5.0). Digital images of the specimens were captured using a Sony DKC-5000, 3 CCD digital camera attached to the microscope and stored on a PC. The magnification, slide number, and orientation of each slide was recorded on paper, in a spreadsheet, as well as through file name and tag. The images were then equalized for white balance and contrast to maximize the image quality, as well as rotated to standardize the orientation of each image. Additionally, microscope rulers were photographed at various magnifications and stored on the PC for measurements.

Sutures each from the wild-type and delayed onset rabbits at 5, 10, 25, 31, 42, and 88 days of age were chosen for histomorphometric analysis. The images selected were picked based on image quality, integrity of the specimen, and availability at the referenced age. In total, 11 unaffected and 15 delayed onset age matched specimens were selected. Using Adobe Photoshop (v 12.0) sutured were traced and outlined with a .3 px white demarcation.

ImageJ (v 1.48) was then used to carry out the metric analysis. For each suture image, the microscope ruler captured at the same magnification was utilized to establish the reference scale in ImageJ. The ruler image was loaded and a 1 mm distance was measured and input into the program to standardize a reference scale for each corresponding magnification.

3.2.1 Qualitative Analysis.

All sutures collected (n=160) were used in an age comparison analysis between the unaffected and DOS rabbits. Generally, the images obtained were used to describe the synostotic foci, the extent of relative bony bridging, and coronal suture morphology in the samples.

3.2.2 Quantitative Metric Data Gathering

The samples selected for histomorphometric analysis were measured using ImageJ to obtain endocortical suture width, mesocortical suture width, ectocortical suture width, total suture area, and number of bony bridges (Figure 2). All measurements were done three times, with the mean measurement being recorded, by the same individual. All measurements were performed at the interdigitating zone as well as at a medially located region of the coronal suture (Figure 1). All measurements were taken blindly with regard to group identity. A random sample of 10% of the images were traced and measured twice. Intra-observer, repeated measurement reliability was calculated at $r = 0.999$; $p < 0.001$, for suture width and $r = 0.988$; $p < 0.001$, for suture area.
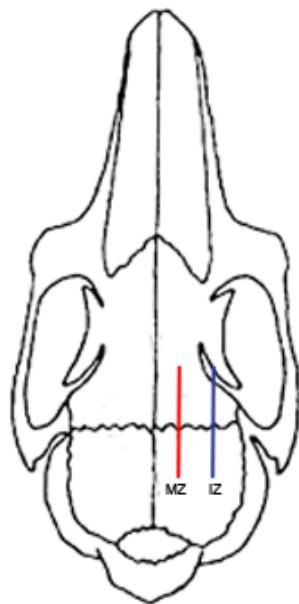
Figure 1 Location of medial (MZ) and interdigitating (IZ) zones.

Suture Area   Suture Width
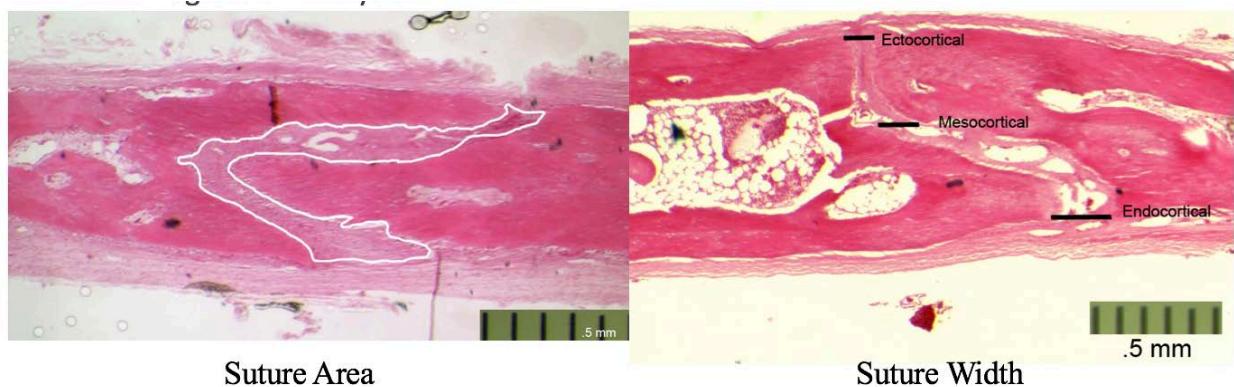
Figure 2 Histophotomicrographs demonstrating the methods of metric data collection

On the left side, the suture has been outlined using Photoshop, and total suture area was measured using ImageJ. The

image on the right shows the levels where suture width was measured.
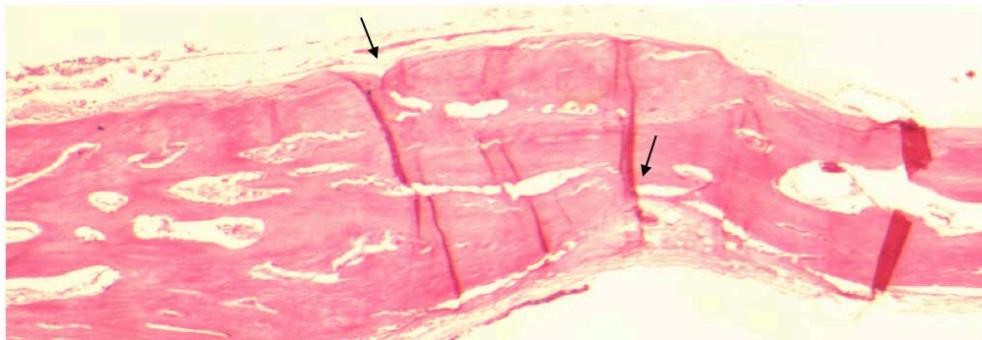
Figure 3 Histophotomicrograph of bony bridging.

3.3   STATISTICAL ANALYSIS

Regression analysis was performed using Microsoft Excel to statistically analyze the data between groups by age. Data was fit to a cubic model, which represents an expected biological growth function. Additional statistical analysis was performed using Using Stata/SE (v 14.2). Unpaired t-test was used to compare the mean suture width and mean total suture area between age matched specimens of each diagnosis group at the ectocortical surface, at the mesocortical level, and at the endocortical surface of the suture at the interdigitating and medial zones. Paired t-test was used to compare the mean number of recorded bony bridges by age group between the interdigitating and medial zones of the DOS affected rabbits. Furthermore, suture width, total suture area, and frequency of bony bridging was analyzed for variance between and within groups using a 6 x 2 (age by group) two-way ANOVA test. Differences were considered significant if $p < .05$.

4.0   RESULTS

4.1   QUALITATIVE ANALYSIS

In wild-type rabbits, the existence of coronal sutures was evident at term and remained patent at all ages. A well defined sutural ligament was present and distinct osteogenic fronts were observed at both the interdigitating and medial zone. The suture showed dorsal-ventral overlapping of the frontal and parietal bones without osseous connections. In the affected (DOS) group, the morphology of the suture resembled the wild type controls until day 10. Initially, specimens from the affected group showed similar suture development and general suture morphology to age match controls sutures from term until day 10. In some DOS sutures, osseous projections, or bony bridges, began to appear at the laterally located interdigitating zone connecting the osteogenic fronts as early as day 10. With increased age, more extensive bony bridging at the interdigitating zone, as well as increased frequency across the suture, was observed. Additionally, sutural ligaments followed a general trend of thickening until day 32 and dramatically narrowing after with associated increase in bony bridging. Typical dorsal-ventral overlapping of the osteogenic fronts was not seen across all ages, with variations ranging from severe overlapping to end to end approximation. Generally, total suture obliteration was observed by day 85. Though general trends and similarities were described, it is worth noting that variance in suture ligament morphology was observed within each age group of the DOS rabbits.
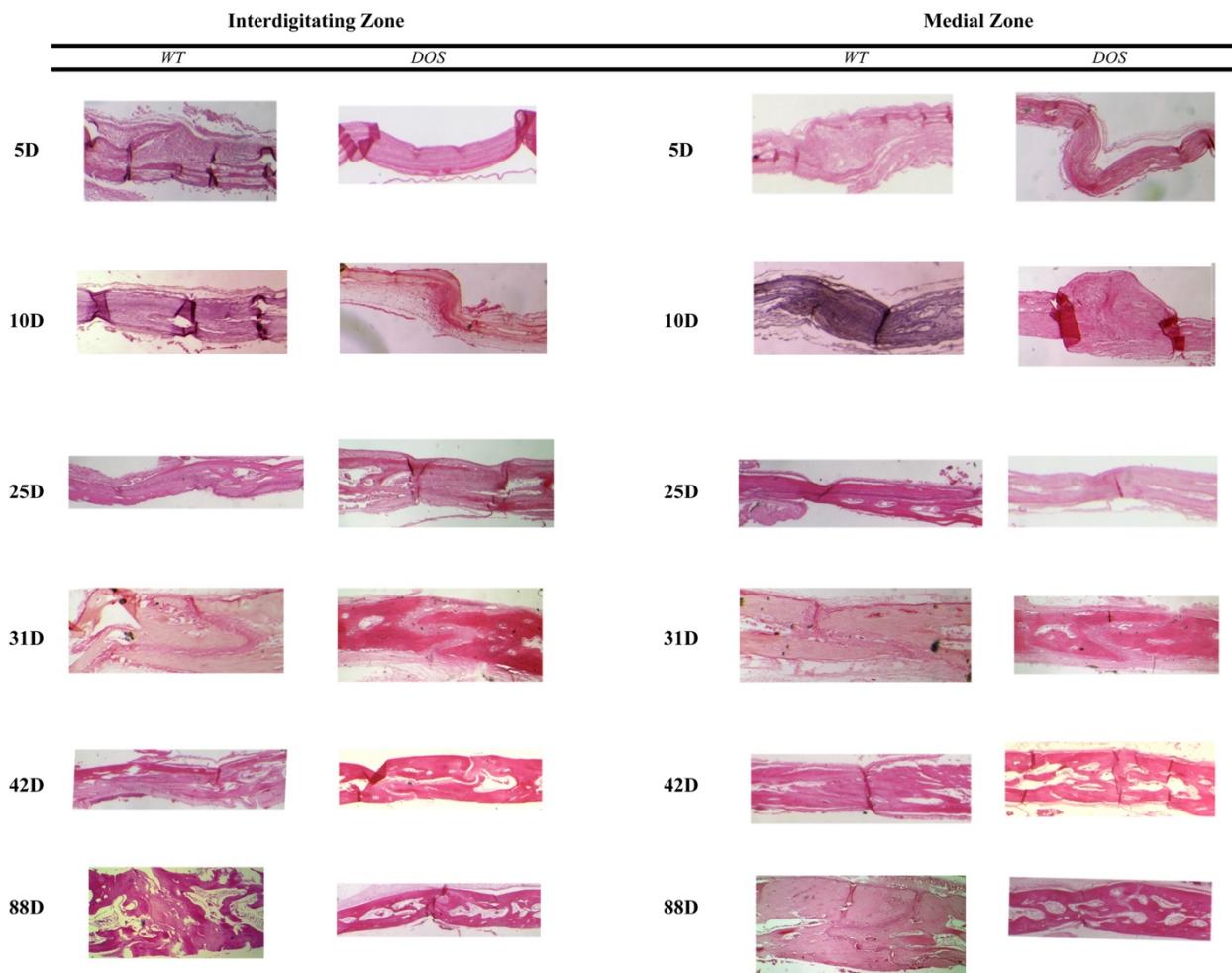
Figure 4 Histophotomicrographs of coronal suture taken from the interdigitating and medial zones from the delayed onset affected animals (DOS) and the wild type controls (WT).

Samples were collected from six different age groups (5-88 days)

4.2   QUANTITATIVE ANALYSIS

4.2.1   Suture Width

4.2.1.1 Interdigitating Zone

Unpaired t-test

To assess potential differences in the morphology of suture at the interdigitating zone of between the wild-type and DOS groups, suture width was measured and analyzed for statistical differences. At the ectocortical, mesocortical, and endocortical surfaces, the coronal suture was measured to be wider in the 5, 10, 25, 45, and 88 days of age rabbits in the wild-type group than the DOS groups. In both groups, suture widths increased slowly from ages 5 to 25 days. In the wild-type group, a rapid growth and expansion of suture width was measured between age 45 and 88. However, in the DOS group coronal suture width plateaued and rapidly narrowed from ages 31 to 88 in days. The maximum mean suture width at all levels of the coronal suture at the interdigitating zone was at age 88 in days in the wild-type group and at age 31 in days in the DOS rabbit group. The unpaired t-test comparing means between the delayed onset group and the age matched wild types at the endocortical, mesocortical, or endocortical surface of the suture showed no significant difference suture width at any age (p >.05) (Tables 2-4).

Table 3 Mean ectocortical suture width measured at the interdigitating zone

		Age (Days)					
		5	*10*	*25*	*31*	*45*	*88*
WT	Mean ± SD	.303 ± .11	0.201	.395 ± .12	0.21	.304 ± .11	.971 ± .51
	n	3	1	2	1	2	2
DOS	Mean ± SD	0.124 ± .07	.15 ± .11	.152 ± .073	0.674 ± .43	.285 ± .15	.197 ± .12
	n	2	2	3	2	4	2
	t-value	-2.060	-	-2.990	-	-0.159	-2.580

* $p < .05$

Table 4 Mean mesocortical suture width measured at the interdigitating zone.

		Age (Days)					
		5	*10*	*25*	*31*	*45*	*88*
WT	Mean ± SD	.199 ± .083	0.178	.425 ± .23	0.185	.377 ± .23	1.0215 ± .41
	n	3	1	2	1	2	2
DOS	Mean ± SD	.076 ± .001	0.114 ± .064	.0933 ± .083	.313 ± .19	.134 ± .10	.1645 ± .03
	n	2	2	3	2	4	2
	t-value	-2.400	-	-2.480	-	-1.910	-2.960

* $p < .05$

16

Table 5 Mean endocortical suture width measured at the interdigitating zone

		Age (Days)					
		5	10	25	31	45	88
WT	Mean ± SD	.25 ± .11	0.184	.408± .22	0.241	.2465 ± .088	1.094 ± .95
	n	3	1	2	1	2	2
DOS	Mean ± SD	.0875 ± .052	.161 ± .09	.093 ± .038	.357 ± .20	.111 ± .067	.176 ± .021
	n	2	2	3	2	4	2
	t-values	-1.870	-	-2.640	-	-2.140	-1.370

* $p < .05$
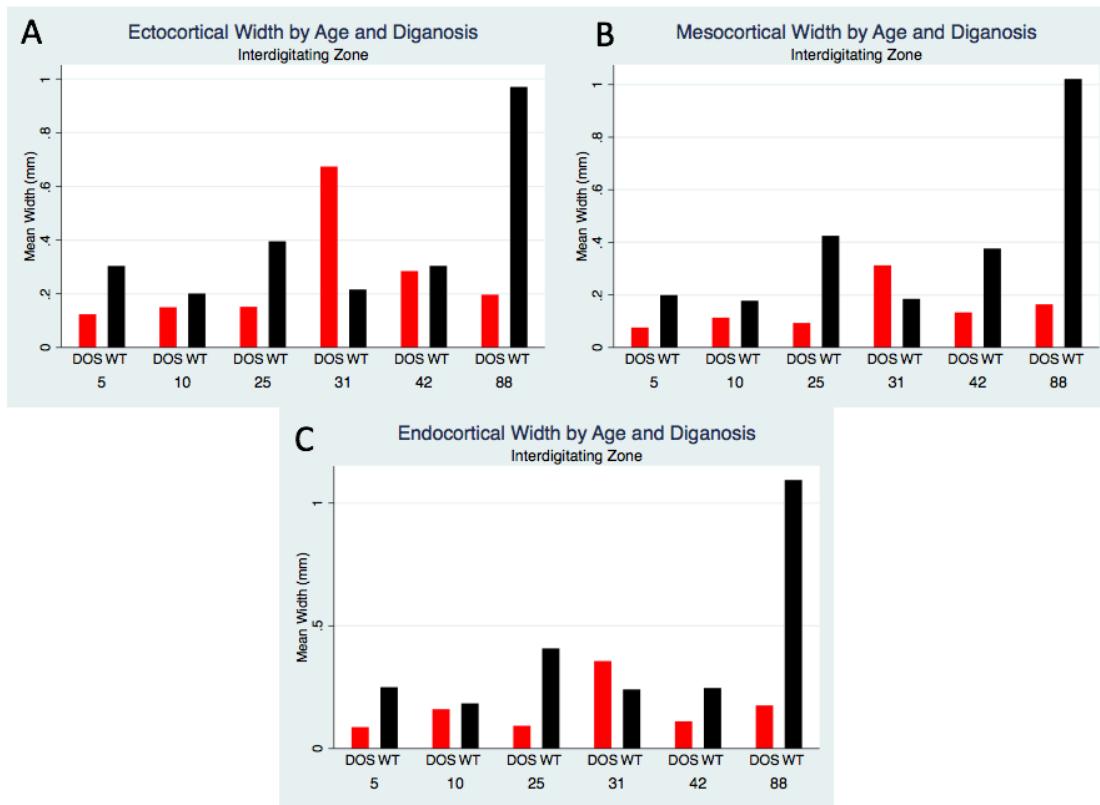
Figure 5 Bar graphs of mean suture width (mm) by group and age at the interdigitating zone.

Bar graphs showing mean suture width at the ectocortical (**A**), mesocortical (**B**), and endocortical (**C**) suture level at the interdigitating zone.

Linear Regression

Linear regression analysis was used to visualize difference in growth rates and patterns in suture width at the interdigitating zone at various levels of the coronal suture. In wild-type group at the ectocortical, mesocortical, and endocortical suture surfaces, a slow growth phase was measured from age 5 to 25 in days. At all three levels, a mild narrowing of the suture occurred between ages 25 and 42 in days which was followed by a rapid growth phase. In comparison, regression curves of the suture width data for the DOS group at the ectocortical surface showed a slower growth rate, leading to a maximum suture width at age 42 in days; this was followed by a rapid depression of growth and narrowing of the suture. A similar trend was seen at the mesocortical and endocortical level of the suture, however, the growth curves generated by the regression analysis of the DOS group is noticeably depressed in comparison to the wild-type controls. Suture width data at the ectocortical level analyzed using a cubic regression model yielded the equation of, $y = 6E\text{-}06x^3 - 0.0006x^2 + 0.0157x + 0.2136$ with an R^2 value of .75 for the wild-type group. The ectocortical suture width data for the DOS group was also applied to a cubic regression model which generated the equation, $y = 2E\text{-}06x^3 - 0.0004x^2 + 0.0211x - 0.0042$, with an R^2 value of .17. At the mesocortical level, the cubic regression analysis for the wild-type group generated a trendline equation of $y = 6E\text{-}06x^3 - 0.0007x^2 + 0.0257x + 0.0754$ with an R^2 value of .74. The DOS suture width data at the mesocortical level cubic regression analysis resulted in an equation of $y = 1E\text{-}06x^3 - 0.0002x^2 + 0.0094x + 0.0317$ with an R^2 of .099. At the endocortical level, cubic regression model applied to suture width data of the wild-type group resulted the trendline equation $y = 9E\text{-}06x^3 - 0.001x^2 + 0.0308x + 0.0975$ with an R^2 values of .53. At the same level in the DOS group, suture width data analyzed using a cubic regression

model generated the equation $y = 3E\text{-}06x^3 - 0.0004x^2 + 0.014x + 0.0321$ with R^2 value of .080

(Figures 6-8).
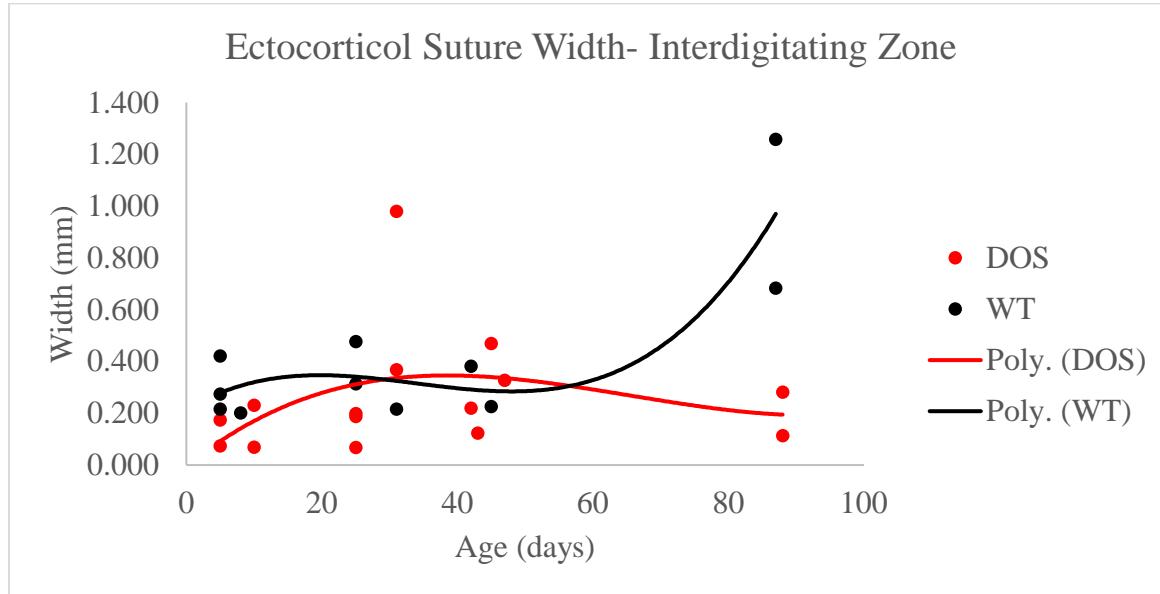
Figure 6 Cubic Regression model of suture width at the ectocortical suture surface at the interdigitating zone.
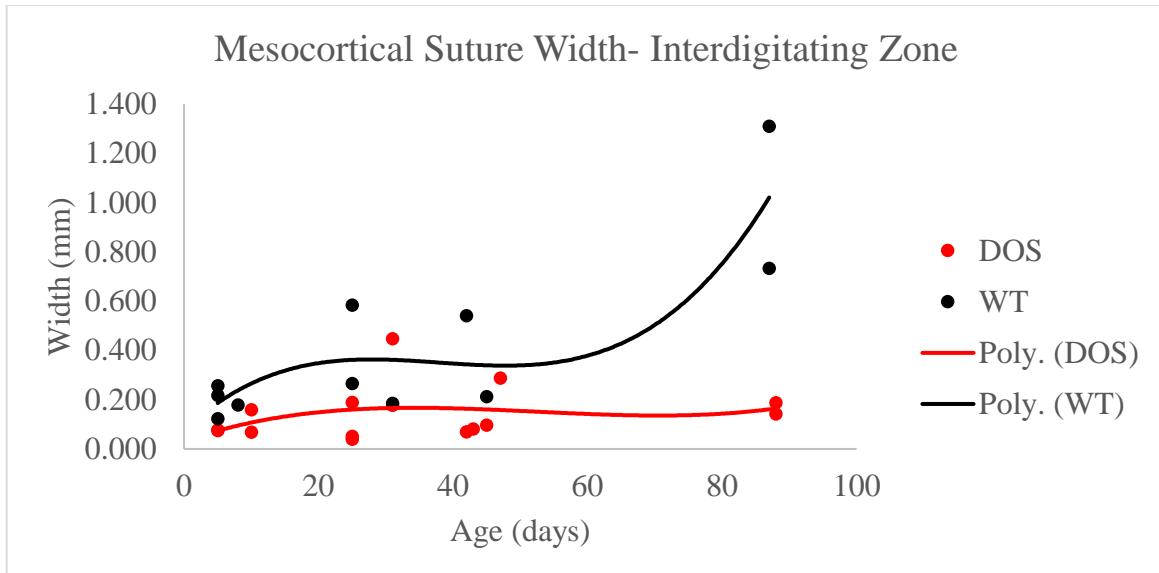
Figure 7 Cubic Regression model of suture width at the mesocortical level of the suture at the interdigitating zone.
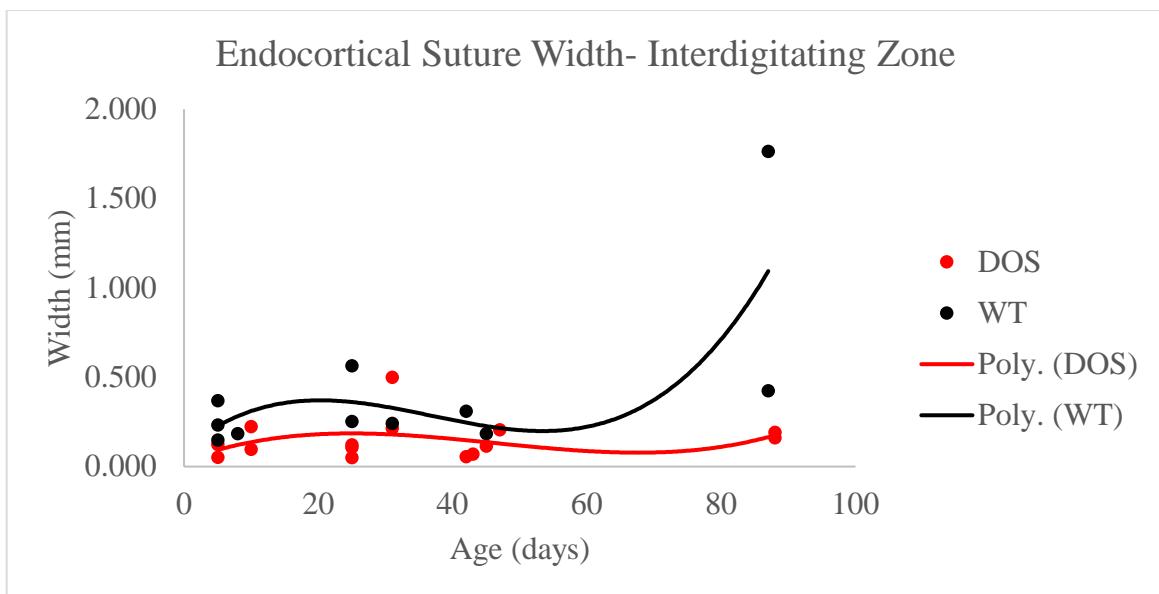
Figure 8 Cubic Regression model of suture width at the endocortical surface of the suture at the interdigitating zone.

4.2.1.2 Medial Zone

Unpaired t-test

Analysis of suture width at the medial zone was performed to determine if any significant measurable differences in suture morphology between the wild-type and DOS groups. In the wild-type group, sutures at the ectocortical surface and mesocortical levels widened from ages 5 to age 25 in days, followed by a brief narrowing period and then a widening period. At the endocortical surface, the widening continued through till age 31 in days, after which, a narrowing was measured at age 45 in days of the collected suture. At all three levels of the suture, a dramatic increase in suture width was measured in sutures collected from the age 88 in days wild-type group. This age group marked the maximum width of the suture measured for the wild-type controls. In the DOS group at the ectocortical surface, the maximum suture width was recorded among the age 31 in day group. Following this peak, a sharp narrowing of the suture was recorded in subsequent age groups at the ectocortical level. In contrast, at the mesocortical level of sutures collected from the DOS rabbits, a moderate increase in width was recorded with increased age groups until age 31 in days. A narrowed suture was recorded in the age 45 in day group, and then an expansion of suture width was recorded in the age 88 in day group. The endocortical surface of the sutures collected from the DOS group recorded slow, steady increasing width with age with exception of a recorded narrowing among the age 25 in day group. The results of the unpaired t-test at the medial zone showed no significant differences in mean suture width at any age at the mesocortical level or at the endocortical suture surface between the wild-type and DOS groups (Tables 7-8). At the ectocortical surface, a difference was found between groups at day 88 (p<.05) (Table 6).

Table 6 Mean ectocortical suture width measure at the medial zone

		Age (Days)					
		5	10	25	31	45	88
WT	Mean ± SD	.107 ± .025	0.076	.311 ± .012	0.295	.156 ± .0042	.554 ± .050*
	n	3	1	2	1	2	2
DOS	Mean ± SD	.1195 ± .067	0.275 ± .053	.196 ± .13	.789 ± .081	.2815 ± .33	0.197 ± .11*
	n	2	2	3	2	4	2
	t-values	0.260	-	-1.180	-	0.503	-4.070*

* $p < .05$

Table 7 Mean mesocortical suture width measured at the medial zone

		Age (Days)					
		5	10	25	31	45	88
WT	Mean ± SD	.104 ± .037	0.110	.255 ± .045	0.227	.133 ± .021	.658 ± .17
	n	3	1	2	1	2	2
DOS	Mean ± SD	.101 ± .024	.174 ± .011	.121 ± .087	.237 ± .066	.159 ± .12	.309 ± .12
	n	2	2	3	2	4	2
	t-values	-0.098	-	-1.940	-	0.293	-2.390

* $p < .05$

Table 8 Mean endocortical suture width measured at the medial zone

		Age (Days)					
		5	10	25	31	45	88
WT	Mean ± SD	.107 ± .043	0.102	.221 ± .011	0.249	.1805 ± .049	.6225 ± .025
	n	3	1	2	1	2	2
DOS	Mean ± SD	.125 ± .067	.148 ± .016	.131 ± .095	.179 ± .028	.195 ± .18	.248 ± .20
	n	2	2	3	2	4	2
	t-values	0.369	-	-1.270	-	0.109	-2.700

* p < .05
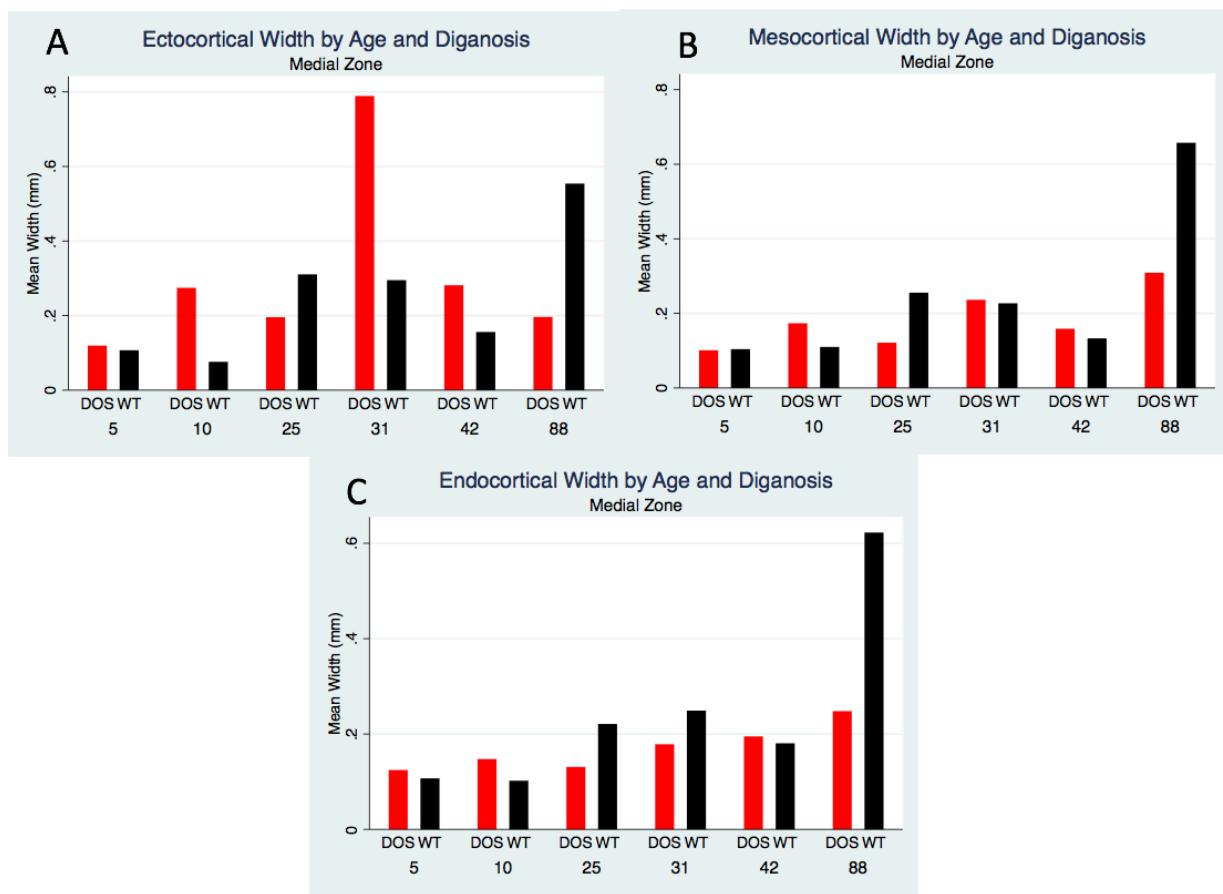
Figure 9 Bar graphs of mean suture width (mm) by group and age at the medial zone.

Bar graphs showing mean suture width at the ectocortical (**A**), mesocortical (**B**), and endocortical (**C**) suture level at the medial zone.

Linear Regression

Regression analysis was applied to suture width data to generate curves representative of the growth rates of the coronal suture at three cortical levels at the medial zone. In the wild-type group, a rapid period of growth is observed at the ectocortical and endocortical surfaces of the coronal suture. At the ectocortical surface, this rapid growth was followed by slower period of suture narrowing until day 60 of age. After this point, another rapid period of growth was observed, leading to maximum suture width by day 88. At the endocortical surface a shallower depression of suture growth rate and less extensive narrowing of the suture was observed after the initial rapid growth phase in the wild-type group. However, an equally rapid phase of growth is represented by regression model. At the mesocortical level, a less dramatic period of growth was seen, and was followed by an equivalent period of slight narrowing of the suture. However, as was seen in at the ectocortical and endocortical levels, a rapid period of suture growth is represented by the cubic regression curve. The regression analysis applied to suture width data collected from the DOS group showed varying trends at each level of the suture. At the ectocortical surface, a rapid growth phase is seen, peaking at approximately 31 days of age. At this cortical level, a long and slow narrowing of the suture follows the rapid growth phase until age 80 in days. The model then indicates another period of growth occurring, though at a relatively depressed rate. At the mesocortical suture level, a slow continuous growth rate is observed until approximately 60 days of age, at which an increase in the rate of suture expansion is seen, with measured suture width peaking at 88 days of age. At the endocortical surface, an initial narrowing of the suture is seen before a slow expansion of the suture peaking at approximately 70 days. However, unlike the ectocortical and mesocortical levels, a plateauing of

24

the suture width followed by narrowing of the suture is observed with an increase in age. For the

wild-type group, suture width data at the ectocortical level analyzed using a cubic regression

model resulted in generation of the equation $y = 9E-06x^3 - 0.0011x^2 + 0.0378x - 0.0759$ with an

R^2 value of .95. At the mesocortical level the equation $y = 4E-06x^3 - 0.0004x^2 + 0.0125x +$

0.0467 was generated, with an R^2 value of .85. At the endocortical suture surface, cubic

regression analysis formulated the equation $y = 5E-06x^3 - 0.0006x^2 + 0.0212x + 0.0059$, with an

R^2 value of .98. In the DOS group at the ectocortical surface, the generated equation was $y = 4E-$

$06x^3 - 0.0006x^2 + 0.0282x + 0.0064$, with an R^2 value of .14. At the mesocortical level, the cubic

regression equation was $y = 1E-06x^3 - 0.0002x^2 + 0.0061x + 0.0922$, with an an R^2 value of .33.

At the endocortical suture surface, the cubic regression equation generated was $y = -2E-06x^3 +$

$0.0002x^2 - 0.0058x + 0.1639$, with an R^2 value of .16 respectively for the DOS affected group.

(Figures 10-12).
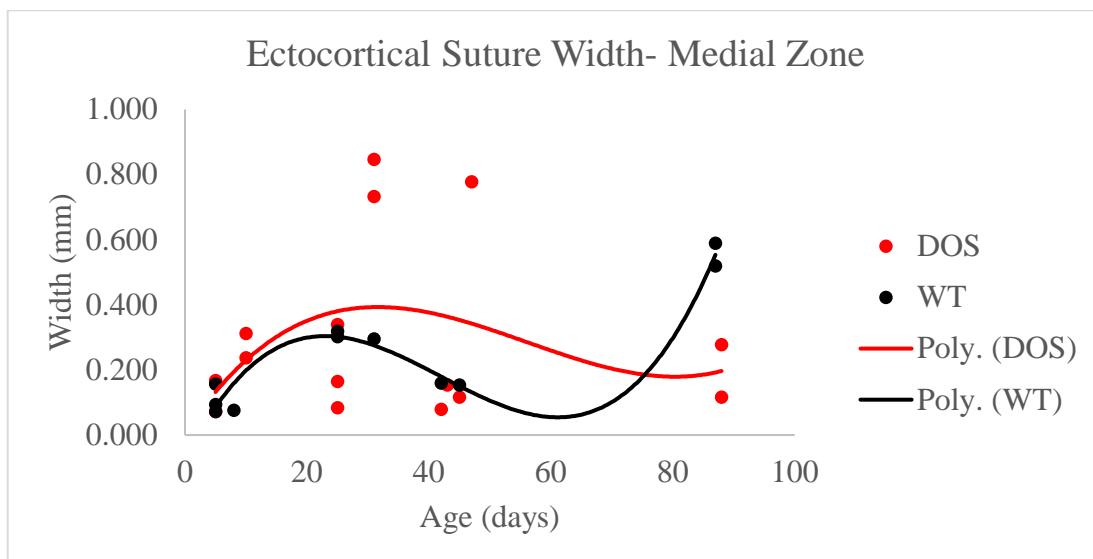
Figure 10 Cubic Regression model of suture width at the ectocortical suture surface at the medial zone.

25
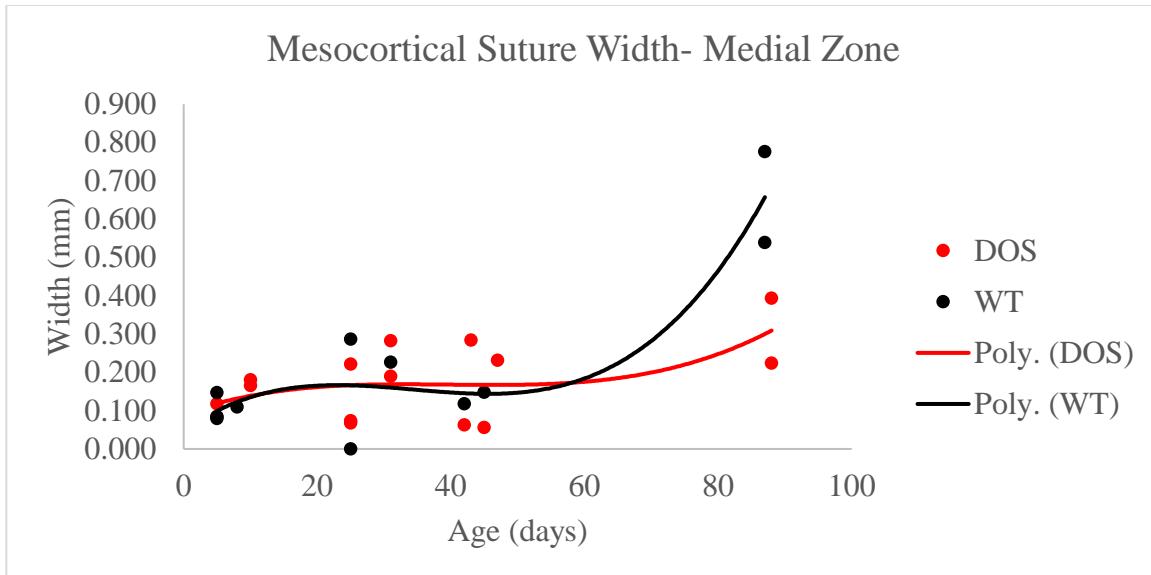
Figure 11 Cubic Regression model of suture width at the mesocortical level of the suture at the medial zone.
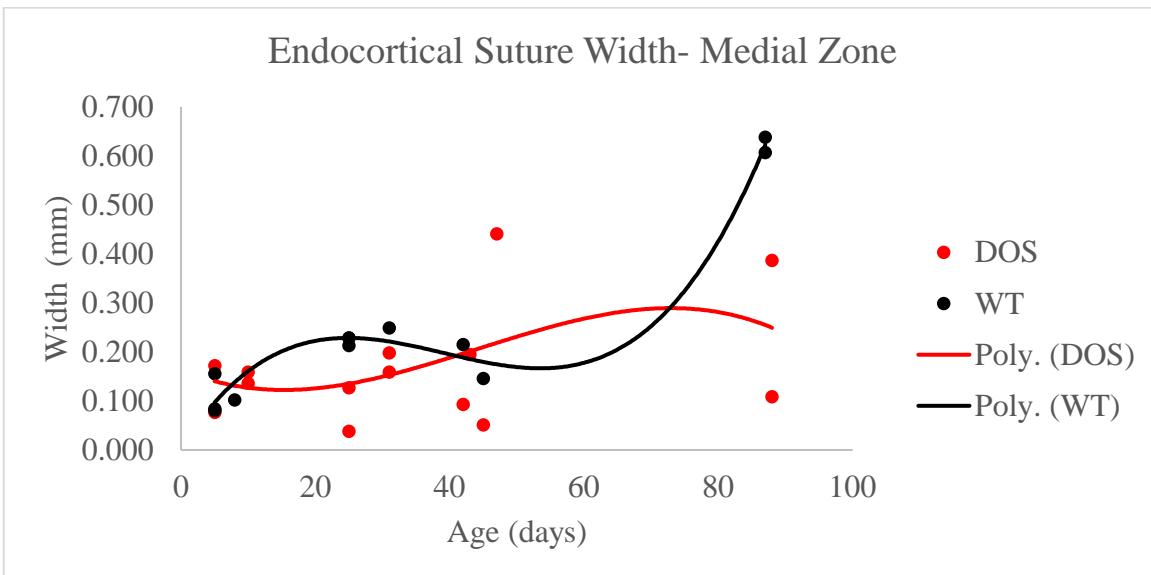
Figure 12 Cubic Regression model of suture width at the endocortical surface of the suture at the medial

zone.

4.2.2　Total Suture Area

4.2.2.1 Interdigitating Zone

In the wild-type group, an increase in total suture area was measured from age 5 to age 45 in days. From age 45 in days to age 88 in days, a dramatic increase in suture area was seen. In the DOS affected group, mean measured total suture area increased until age 31 in days. Following this age group, a reduction in suture area was recorded, followed by a moderate expansion of suture area by age 88 in days. No significant difference was found in mean suture area at any age group measured at the interdigitating zone ($p > 0.05$) (Table 9).

Table 9 Mean total suture area (mm^2) by age group measured at the interdigitating zone

		Age (Days)					
		5	*10*	*25*	*31*	*45*	*88*
WT	Mean ± SD	.11 ± .013	0.034	.18 ± .094	0.193	.213 ± .11	1.305 ± .75
	n	3	1	2	1	2	2
DOS	Mean ± SD	.089 ± .098	.057 ± .025	.065 ± .071	.221 ± .0099	.12 ± .075	.27 ± .055
	n	2	2	3	2	4	2
	t-values	-0.439	-	-2.290	-	-1.320	-1.950

* $p < .05$

27

4.2.2.2 Medial Zone

Total suture area in the wild-type group showed a measured increase in suture area with progression of age until age 45 in days. The 45 day old samples indicate a narrowing of suture area, which was followed by an increase measured total suture area in the 88 days old group. Among the DOS group, total suture area remained consistent between the 5, 10, and 25 days in age groups. However, an increase of suture area was measured in the 31 day age group. Subsequent total suture area measurements indicate a plateauing of suture area.   At the medial zone, statistically significant differences were found among the 25 day and 88 day age groups (p <.05) (Table 10).

Table 10 Mean total suture area (mm^2) by age group measured at the medial zone

| | | Age (Days) | | | | | |
		5	*10*	*25*	*31*	*45*	*88*
WT	Mean ± SD	.029 ± .015	0.029	.079 ± .0035*	0.160	.094 ± .035	.52 ± .064*
	n	3	1	2	1	2	2
DOS	Mean ± SD	.055 ± .051	.032 ± .0028	.032 ± .0075*	.207 ± .041	.23 ± .13	.23 ± .047*
	n	2	2	3	2	4	2
	t-values	0.887	-	-7.820	-	1.410	-5.204*

* p < .05

28

4.2.3 Bony Bridging

At the interdigitating zone, bony bridging appeared first at a sample that was 10 days of age in the partially affected animal. Observation of bony bridging increased within the 25 day rabbits (5 bony bridges recorded for n=3 rabbits) and was maximally observed at 42 day affected rabbits (11 bony bridges for n=4 rabbits). The unaffected rabbits did not show any bony bridging between the frontal and parietal bones at any age.

At the medial located zone of observation bony bridging was first recorded in one sample of 25 day old affected rabbits in the medial region of the coronal suture. One bony bridge was recorded among the two 32 day samples, and two bony bridges were observed among the four 42 day old samples. By day 88, more extensive bony bridging was observed in the coronal sutures of the affected rabbits. No sutures of the unaffected control animals showed bony bridging at any age group.

Table 11 Mean frequency of recorded bony bridges between the frontal and parietal bone recorded at the interdigitating and medial zones.

		Age (Days)					
		5	10	25	31	45	88
IZ	Mean ± SD	0	.5 ± .71	1.67 ± 2.08	.5 ± .71	2.75 ± .96*	3.0 ± 0.0
	n	2	2	3	2	4	2
MZ	Mean ± SD	0	0.000	.33 ± .58	.5 ± .71	.5 ± .58*	1.5 ± .71
	n	2	2	3	2	4	2

* $p < .05$

4.2.4   6 X 2 (Age by group) two-way ANOVA

The results of the two-way ANOVA indicate significant interaction between age and group for suture width measured at the interdigitating zone at the ectocortical and mesocortical level of the suture as well as for total suture area (p<.05) was found (Table 12). At the medial zone, two-way ANOVA revealed significant interaction between age and group was found with suture width at the mesocortical level and total suture area (p<.05) (Table 12). At the interdigitating zone, a significant fixed effect of age on mesocortical suture width and total suture area was found (p<.05). Additionally at the interdigitating zone diagnosis group was found to have a significant effect on mesocortical and endocortical suture width, total suture area, and frequency of bony bridging (p<.05). At the medial zone, age had a significant fixed effect on endocortical suture width (p<.05), mesocortical suture width (p<.001), and total suture area (p<.001). Diagnosis group showed a significant effect on frequency of bony bridging at the medial zone (p<.05).

Table 12 Results of 6 X 2 (age by group) two-way ANOVA for suture width, total suture area, and frequency

of bony bridging. *p < .001. **p <.05.

		F Values		
		Age	*Group*	*Age x Group*
	Suture Width:			
	Ectocortical	2.43	2.81	3.7**
Interdigitating Zone	Mesocortical	4.14**	13.18**	3.87**
	Endocortical	1.75	4.32	1.6
	Total Suture Area	6.87**	5.29**	3.75**
	Frequency of Bony Bridges	1.89	12.45**	1.89
	Suture Width:			
	Ectocortical	2.79	0.7	2.46
Medial Zone	Mesocortical	10.09*	3	2.99**
	Endocortical	4.76**	2.85	2.1
	Total Suture Area	15.87*	0.57	5.19**
	Frequency of Bony Bridges	1.57	6.57**	1.57

p <.001 *
p < .05**

5.0   DISCUSSION

The present study was designed to describe and quantify the morphology of the coronal suture in rabbits affected with delayed onset craniosynostosis against age matched controls as well as to highlight key features of the progression of suture fusion. In both groups, a patent suture consisting of a regular and uniform sutural ligament and normal dorsal-ventral overlapping of osteogenic fronts were seen in sutures at days 0-10 of age. In some DOS specimens, suture fusion was seen as early ten days. Extensive bony bridging was observed in most DOS sutures by day 42. In such cases, bony bridging between the frontal and parietal osteogenic fronts were observed and may serve as initiation foci for suture closure. Bony bridging increased with age in the DOS affected specimens, and was generally observed at the interdigitating zone at earlier ages than at the medial zone. The interdigitating zone has previously been described as a synostotic foci in sutures collected from rabbits affected with early onset coronal suture craniosynostosis (Mooney et al., 1996). Additionally, suture fusion was reported to progress medially and laterally with increased gestational age in the early onset craniosynostosis phenotype (Mooney et al., 1996). Tensile biomechanical forces occurring with normal skull growth are increased at the location of the suture where the interdigitating zone has been described, and may account for the initiation of synostosis occurring at this location (Herring 2000; Mooney et al., 1996).

With an increase in age, several other key differences were noted between sutures of the delayed onset and age matched wild type controls. Normal dorsal ventral overlapping of the osteogenic fronts was often not observed in sutures past day 10 in the delayed onset group.

Typically, end to end approximation of the bones was observed, and the osteogenic fronts were noticeably thicker in the DOS sutures when compared to sutures collected from the control group. In addition to regular overlapping of osteogenic fronts, wild type sutures consisted of a sutural ligament uniform in width and morphology at all ages. In the sutures analyzed from the DOS affected group, the sutural ligament began appearing dysmorphic and irregular approximately by day ten. The changes were most commonly seen first at the endocortical surface of sutures collected from the affected group. The narrowing and disappearance of the sutural ligament in conjunction with extensive bony bridging suggests that initial mechanical fusion of the coronal suture in DOS affected mostly occurs between 32 and 42 days after birth. This may indicate a change in the genetic and molecular environment at this timeframe causing leading to an increase in bone deposition and the initial stages of suture fusion. A previous study using amalgam markers to track separation of the coronal suture in DOS affected animals showed a marked decrease in growth by six weeks and continued depression when compared to wild-type control groups (Mooney et al., 1994b). This coincides with the timeline of changes observed at a histological level of affected sutures. By day 88, most sutures collected from DOS animals showed complete suture fusion with loss of a distinct sutural ligament and ectocortical ridging at the site of approximation; in wild-type controls, sutures remained patent.

Progression of synostosis of sutures in the DOS affected group was not uniform across all specimens of the same age group. A high degree of variance in phenotypic expression and course timeline of pathologies suggests heterogeneity amongst the group clustered together as delayed onset. Further investigation is needed to categorize and describe phenotypic variations of suture fusion progression within the affected group used in this study.

The metric analysis of the collected coronal sutures focused on measuring suture width (ectocortical, mesocortical, and endocortical levels), total suture area, and frequency of bony bridging at both the interdigitating zone and medial zone of DOS and WT sutures. The unpaired t-test comparing means suture widths at various levels only showed a significant difference between the two groups at the ectocortical suture surface at the medial zone among 88 day old specimens ($p<.05$) (Tables 3-8). However, the suture width data suggests an overall narrowing of the suture in affected animals in comparison to age matched controls. Additionally, it is important to note the relative consistency in suture width at the ectocortical, mesocortical, and endocortical levels among the wild type controls against the variability in width along the thickness of the suture observed in the samples collected from the DOS subjects (Tables 2-7). Suture width data at the interdigitating zone indicates that an initial formation of the suture does occur, however, in comparison to the wild type controls, depressed growth and an eventual plateauing of suture widening occurs at approximately 42 days of age. This depression and eventual cessation of suture growth is seen more extensively at the endocortical surface at the interdigitating zone than other cortical surfaces. This may be due to the proximity of the dural tracts and stronger influence of molecular signals on bone deposition. At the medial zone, suture width plateauing and reduction was also observed, however, the morphological changes were observed later than at the interdigitating zone. This further indicates that synostosis begins at the interdigitating zone and progresses across the span of the suture.

Comparison of mean total suture area at various age points did not reveal significant differences between the groups at the interdigitating zone; this may be attributed to the general dysmorphic shape of the sutural ligament seen in the DOS sutures. However, analysis of

34

measurements made at the medial zone indicates significant differences at ages 25 and 88 between the groups (Table 10). It is important to note that the statistical differences in total suture area measured at the medial zone does not infer this site along the suture as the initiation foci of synostosis; instead the data should be interpreted as indications of suture morphology differences between the affected and unaffected groups. For metric investigation of the synostosis foci, mean frequency of bony bridging between the interdigitating and medial zones (Table 11). The significant ($p<.05$) difference and increased frequency of recorded bony bridging at day 45 suggests the interdigitating zone as the site of suture fusion initiation, as was previously described in rabbits from this colony with early onset congenital craniosynostosis (Mooney et al., 1996).

The regression analysis of the suture width data was conducted can be used to describe growth trends at the interdigitating and medial zone at three different levels of the suture thickness. A cubic regression model was used to describe the wild type suture data because it yielded the higher R^2 values than other models, suggesting the data was best fit to a cubic regression analysis. This also indicates a biphasic growth pattern consisting of an initial rapid widening phase, an intermediate period of narrowing, and a secondary phase of rapid widening along the suture (Figure 6-8, 10-12). With the same model applied to data collected from the affected group, suture width at the interdigitating zone consisted of a slow widening phase peaking between 20 and 45 days followed by dramatically reduced suture width with progression of age (Figures 6-8). This suggests initial development of a patent suture may be present, however, decreased growth rates as well as a plateauing of suture development may be observed.

This pattern was similarly described using amalgam markers to track separation of partial synostosis coronal sutures (Mooney et al., 1994b).

An estimated 300 per 1 million babies born are affected with nonsyndromic craniosynostosis, of which 24% involve the coronal suture (Cohen 1986). Nonsyndromic delayed onset craniosynostosis was described in a human case study (Cohen et al., 1993) as well as in association with Crouzon syndrome, Saethre-Chotzen syndrome, Pfeiffer syndrome, and other syndromic cases (Rogers et al., 2015; Cohen, 2000c, Connolly et al., 2004, Hoefkens et al., 2004). Though delayed-onset synostosis has been diagnosed in a small number of patients, it is important to consider the potential for under reporting of affected individuals. Individuals with delayed-onset craniosynostosis may only experience mild symptoms or even present as asymptomatic if the process occurs following the cessation of major brain growth and development.

Affected patients often present with intellectual development abnormalities, cosmetic and anatomical defects, cognitive impairments, and elevated intracranial pressure (Connolly et al., 2004, Scott et al., 2009). Surgical corrective measures and remodeling helmets, the gold standard of treatment, are necessary to avoid dangerous risks associated with leaving a patient untreated (Governale, 2015). However, the treatment itself is limited by complications of the surgery and need for continual correction to relieve symptoms of elevated intracranial pressure (Jane et al., 2015; Scott et al., 2009). The biochemical pathogenesis of suture fusion is not fully understood, however, recent studies have made major strides in uncovering the roles of local tissue factors in suture physiology and pathology (Cohen, 2000). For example, signaling from the dura mater has

been associated with regulating suture patency (Opperman et al., 1993, 1995). In affected rabbits, dura mater cells showed abnormal rapid proliferation as well as associated increased influence of bone cell differentiation (Cooper et al., 2012). Signaling cytokines groups secreted from the dura mater, such as the Tgf-β family, have been explored for their role in suture fusion as well as potential therapeutic uses.   Injections of one isoform, TGF- β3, may have clinical applications as therapy to rescue sutures in delayed onset craniosynostosis as well as delay reossification following surgical correction of fused coronal sutures. (Chong et al., 2003; Gilbert et al., 2016). In rabbits with delayed onset craniosynostosis associated elevation of TGF- β2 is also seen (Cohen 2000; Poisson et al., 2004).   An antagonistic suppression of TGF-β2 using neutralizing antibodies also shows potential therapeutic application in preventing the progression of suture fusion in delayed onset craniosynostosis (Mooney et al, 2016). Additionally, the role of bone morphogenic protein in suture fusion has been investigated; one studied found a direct effect of rhBMP-2 on coronal suture fusion (Kinsella et al., 2011).

To find other potential treatment options, further investigations of etiological factors and the pathogenesis contributing to abnormal suture fusion must be performed. The progression of suture fusion described in this study is similar to that described in prenatal suture fusion (Mooney et al., 1996). Additional studies comparing the two phenotypic expressions (complete and delayed onset) of non syndromic craniosynostosis should be conducted to determine if the delay-onset variant serves as an adequate model for preterm suture fusion. The variations and heterogeneity of the sutural morphology observed should also be explored for potential links and commonalities for a more comprehensive understanding of the morphological events and changes that occur during suture fusion in delayed onset of craniosynostosis.

T-VALUES

Table 13 t-values from all unpaired t-tests performed

		t-values					
		5	*10*	*25*	*31*	*45*	*88*
	Suture Width						
	Ectocortical	-2.060	-	-2.990	-	-0.159	-2.580
IZ	*Mesocortical*	-2.400	-	-2.480	-	-1.910	-2.960
	Endocortical	-1.870	-	-2.640	-	-2.140	-1.370
	Total Suture Area	-0.439	-	-2.290	-	-1.320	-1.950
	Suture Width						
	Ectocortical	0.260	-	-1.180	-	0.503	-4.070
MZ	*Mesocortical*	-0.098	-	-1.940	-	0.293	-2.390
	Endocortical	0.369	-	-1.270	-	0.109	-2.700
	Total Suture Area	0.887	-	-7.820	-	1.410	-5.204

BIBLIOGRAPHY

Chong, S.L., et al., Rescue of coronal suture fusion using transforming growth factor-beta 3 (Tgf-beta 3) in rabbits with delayed-onset craniosynostosis. *Anat Rec A Discov Mol Cell Evol Biol*, 2003. 274(2): p. 962-71.

Chumas, P.D., et al., Classification of previously unclassified cases of craniosynostosis. *J Neurosurg*, 1997. 86(2): p. 177-81.

Cohen, M. M., Jr. Epidemiology of craniosynostosis. In M. M. Cohen, Jr., and R. E. MacLean (Eds.), *Craniosynostosis: Diagnosis, Evaluation, and Management.* New York: Oxford University Press, 2000. Pp. 112–118.

Cohen, M. M., Jr. Sutural biology. In M. M. Cohen, Jr., and R. E. MacLean (Eds.), *Craniosynostosis: Diagnosis, Evaluation,and Management.* New York: Oxford University Press, 2000. Pp. 11–23.

Cohen, M. M., Jr. Sutural pathology. In M. M. Cohen, Jr., and R. E. MacLean (Eds.), *Craniosynostosis: Diagnosis, Evaluation, and Management.* New York: Oxford University Press, 2000. Pp. 95–99.

Cohen M.M., Jr. Sutural biology and the correlates of craniosynostosis. *Am J Med Genet* 1993; 47:581–616

Cohen SR, Dauser RC, Gorski JL. Insidious onset of familial craniosynostosis. *The Cleft palate-craniofacial journal : official publication of the American Cleft Palate-Craniofacial Association*. 1993;30(4):401-5.

Connolly, J.P., et al., Progressive postnatal craniosynostosis and increased intracranial pressure. *Plast Reconstr Surg*, 2004. 113(5): p. 1313-23.

Cooper, G. M., Durham E. L., Cray J. J., Siegel M. I., Losee J. E., and Mooney M. P., "Tissue interactions between craniosynostotic dura mater and bone," *Journal of Craniofacial Surgery*, vol. 23, no. 3, pp. 919–924, 2012.

Cunningham, M., Heike, C., Evaluation of the infant with an abnormal skull shape. *Current Opinion Pediatr*, 2007. *19:*645-651.

de Ribaupierre, S., et al., Frontosphenoidal synostosis: a rare cause of unilateral anterior plagiocephaly. *Childs Nerv Syst*, 2007. 23(12): p. 1431-8.

Francel, P.C., et al., Frontal plagiocephaly secondary to synostosis of the frontosphenoidal suture. Case report. *J Neurosurg*, 1995. 83(4): p. 733-6.

Gilbert, J., et al., Transforming Growth Factor-beta3 Therapy Delays Postoperative Reossification and Improves Craniofacial Growth in Craniosynostotic Rabbits. *Cleft Palate Craniofac J*, 2016. 53(2): p. 210-21.

Gilbert, J.R., et al., Genetic Homozygosity and Phenotypic Variability in Craniosynostotic Rabbits. *Cleft Palate Craniofac J*, 2016.

Governale, L.S., Craniosynostosis. *Pediatr Neurol*, 2015. 53(5): p. 394-401.

Graham J.M. Jr, Badura R.J., Smith D.W., Coronal craniostenosis: fetal head constraint as one possible cause. *Pediatrics* 1980; 65:995–999.

Greene, A.K., et al., Phenotypically unusual combined craniosynostoses: presentation and management. *Plast Reconstr Surg*, 2008. 122(3): p. 853-62.

Herring, S.W. Sutures and Craniosynostosis: A Comparative, Functional, and Evolutionary Perspective. In M. M. Cohen, Jr., and R. E. MacLean (Eds.), *Craniosynostosis: Diagnosis, Evaluation,and Management.* New York: Oxford University Press, 2000. Pp. 3–10.

Herring, S.W., Mechanical influences on suture development and patency. *Front Oral Biol*, 2008. 12: p. 41-56.

Hoefkens, M.F., C. Vermeij-Keers, and J.M. Vaandrager, Crouzon syndrome: phenotypic signs and symptoms of the postnatally expressed subtype. *J Craniofac Surg*, 2004. 15(2): p. 233-40; discussion 241-2.

Jane, J.A., Jr., M.D. Krieger, and J. Persing, Introduction: craniosynostosis: modern treatment strategies. *Neurosurg Focus*, 2015. 38(5): p. E1.

Johnson D, Wall SA, Mann S, Wilkie AO. A novel mutation, Ala315Ser, in FGFR2: a gene-environment interaction leading to craniosynostosis? *Eur J Hum Genet* 2000; 8:571–577.

Johnson D, Wilkie A.O., Craniosynostosis. *Eur J Human Gen.*2011; 19:369-376

Kinsella, C.R., Jr., et al., Recombinant human bone morphogenetic protein-2-induced craniosynostosis and growth restriction in the immature skeleton. *Plast Reconstr Surg*, 2011. 127(3): p. 1173-81.

Mooney M, Losken H, Tschakaloff A, Siegel M, Losken A, and Lalikos J (1993) Congenital bilateral coronal suture synostosis in a rabbit and craniofacial growth comparisons with experimental models. *Cleft Palate-Craniofacial Journal 30:*121-128.

Mooney, M.P., et al., Craniosynostosis with autosomal dominant transmission in New Zealand white rabbits. *J Craniofac Genet Dev Biol*, 1996. 16(1): p. 52-63.

Mooney, M.P., et al., Rescue of Premature Coronal Suture Fusion With TGF-beta2 Neutralizing Antibody in Rabbits With Delayed-Onset Synostosis. *Cleft Palate Craniofac J*, 2016.

Mooney M, Siegel M, Burrows A, Smith T, Losken H, Dechant J, Cooper G, and Kapucu M (1998) A rabbit model of human familial, nonsyndromic unicoronal suture synostosis. Part I: Synostotic onset, pathology, and sutural growth patterns. *Child's Nervous System 14:*236-246

Mooney M, Losken H, Siegel M, Lalikos J, Losken A, Burrows A, and Smith T (1994a) Development of a strain of rabbits with congenital simple, nonsyndromic coronal suture synostosis. Part I: Breeding demographics, inheritance pattern, and craniofacial anomalies. *Cleft Palate-Craniofacial Journal 31:*1-7

Mooney M, Losken H, Siegel M, Lalikos J, Losken A, Burrows A, and Smith T (1994b) Development of a strain of rabbits with congenital simple, nonsyndromic coronal suture synostosis. Part II: Somatic and craniofacial growth patterns. *Cleft Palate-Craniofacial Journal 31:*8-16

Mooney, M.P., Reed, J.C., Kovacik M.E., Barbano, T., Cooper, G.M., Losee, J.E., Siegel, M.I. Dural track morphology in rabbits with premature coronal suture fusion. *J. Dental Research*, 2007: 86, Special Issue A; 762.

Mooney MP, Smith TD, Burrows AM, et al. Coronal suture pathology and synostotic progression in rabbits with congenital craniosynostosis. *Cleft Palate Craniofac J* 1996;33:369Y378

Opperman, L.A., et al., Cranial sutures require tissue interactions with dura mater to resist osseous obliteration in vitro. *J Bone Miner Res*, 1995. 10(12): p. 1978-87.

Opperman, L.A., et al., Tissue interactions with underlying dura mater inhibit osseous obliteration of developing cranial sutures. *Dev Dyn*, 1993. 198(4): p. 312-22.

Poisson, E., Sciote, J. J., Koepsel, R., Cooper, G. M., Opper- man, L. A., and Mooney, M. P. Transforming growth factor- beta isoform expression in the perisutural tissues of cranio-synostotic rabbits. *Cleft Palate Craniofac. J.* 41: 392, 2004.

Reardon W, Wilkes D, Rutland P, et al. Craniosynostosis associated with FGFR3pro250arg mutation results in a range of clinical presentations including unisutural sporadic craniosynostosis. *J Med Genet* 1997; 34:632– 636.

Reddy K, Hoffman H, Armstrong D. Delayed and progressive multiple suture craniosynostosis. *Neurosurgery*. 1990;26(3):442-8.

Reed, J.C., Kovacik, M.E., Barbano T.E., Siegel, M.I., Mooney, M.P. Polarized light microscopy of the dural tracks underlying prematurely synostosed coronal sutures in New Zealand white rabbits. *Amer. J. of Physical Anthropologists*, 2007; Supplement 44: 196.

Renier D, El-Ghouzzi V, Bonaventure J, et al. Fibroblast growth factor receptor 3 mutation in nonsyndromic coronal synostosis: clinical spectrum, prevalence, and surgical outcome. *J Neurosurg 2000*; 92:631–636.

Rogers, G.F., et al., Progressive Postnatal Pansynostosis. *Cleft Palate Craniofac J*, 2015. 52(6): p. 751-7.

Seto ML, Hing AV, Chang J, et al. Isolated sagittal and coronal craniosynos- tosis associated with TWIST box mutations. *Am J Med Genet A 2007*; 143:678 – 686.

Scott, J.R., et al., Symptom outcomes following cranial vault expansion for craniosynostosis in children older than 2 years. *Plast Reconstr Surg*, 2009. 123(1): p. 289-97; discussion 298-9.